Supplemental Materials for

DECODING PAIN: UNCOVERING THE FACTORS THAT AFFECT PERFORMANCE OF NEUROIMAGING-BASED PAIN MODELS

Dong Hee Lee[1,2,3], Sungwoo Lee[1,2,3], Choong-Wan Woo[1,2,3]

[1] Center for Neuroscience Imaging Research, Institute for Basic Science, South Korea
[2] Department of Biomedical Engineering, Sungkyunkwan University, South Korea
[3] Department of Intelligent Precision Healthcare Convergence, Sungkyunkwan University, South Korea

This PDF file includes:

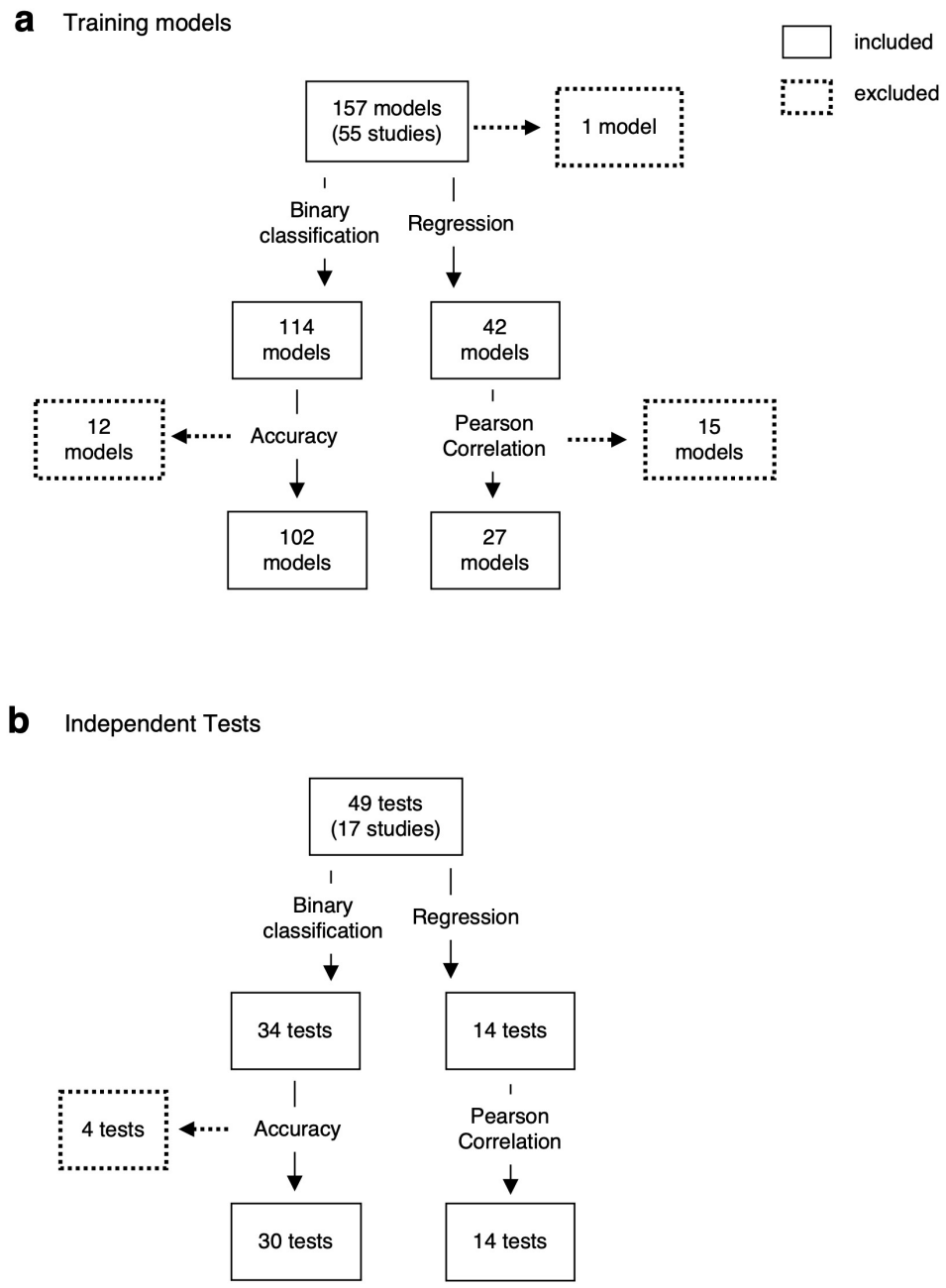

Figure S1. Selection Flowchart for Training Models and Independent Tests. This flowchart details the criteria and process for the inclusion of (a) training models and (b) independent tests from the literature survey. We included training models and independent tests that reported accuracy using classification accuracy or Pearson correlations. The boxes with solid lines indicate the number of test performances included in the survey. The boxes with dotted lines indicate the number of test performances excluded from the survey, which included measures such as sensitivity or mean squared error. Also, we excluded one multi-class classification task from the training model

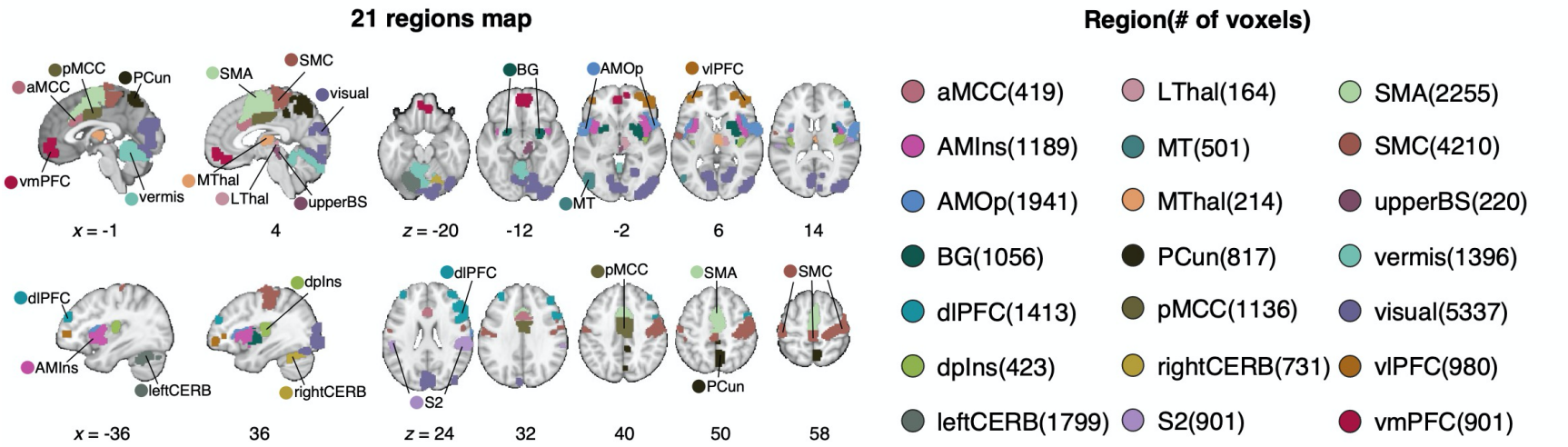

Figure S2. Pre-defined 21 pain-predictive regions. We used pre-defined regions-of-interest (ROIs) that were identified from a previous study [21]. On the left, colored areas illustrate the spatial extent of the brain regions. Each region included a different number of voxels, which is provided on the right. aMCC, anterior midcingulate cortex; AMIns, anterior middle insula; AMOp, anterior middle operculum; BG, basal ganglia; dlPFC, dorsal lateral prefrontal cortex; dpIns, dorsal posterior insula; leftCERB, left cerebellum; LThal, lateral thalamus; MT, middle temporal area; MThal, middle thalamus; PCun, precuneus; pMCC, posterior midcingulate cortex; rightCERB, right cerebellum; S2, secondary somatosensory cortex; SMA, supplementary motor area; SMC, sensorimotor cortex; upperBS, upper brainstem; visual, visual cortex; vlPFC, ventrolateral prefrontal cortex; vmPFC, ventromedial prefrontal cortex.

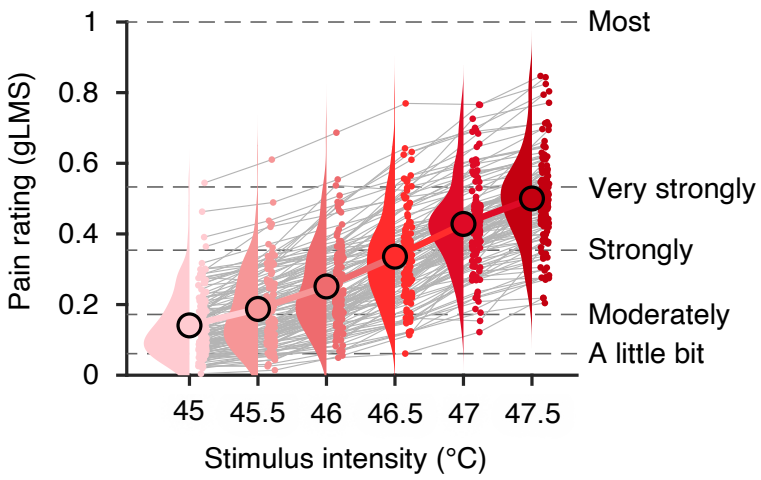

Figure S3. Pain intensity ratings for different levels of stimulus intensity. Each dot represents a mean pain intensity rating for each participant and for each stimulus intensity level. Each line connecting dots represents the pain ratings of one individual. We used the generalized Labeled Magnitude Scale (gLMS) for pain ratings (y-axis).

Table S1. BEST (Biomarkers, EndpointS, and other Tools) biomarker terminology and definitions

Type	Definition
Diagnostic	To detect or confirm presence of a disease or condition of interest or to identify individuals with a subtype of the disease.
Predictive	To identify individuals who are more likely than similar individuals without the biomarker to experience a favorable or unfavorable effect from exposure to a medical product or an environmental agent.
Prognostic	To identify likelihood of a clinical event, disease recurrence or progression in patients who have the disease or medical condition of interest.
Safety	Measured before or after an exposure to a medical product or an environmental agent to indicate the likelihood, presence, or extent of toxicity as an adverse effect.
Pharmacodynamic/ Response	To show that a biological response has occurred in an individual who has been exposed to a medical product or an environmental agent.
Monitoring	Measured serially for assessing status of a disease or medical condition or for evidence of exposure to (or effect of) a medical product or an environmental agent.
Susceptibility/ Risk	Potential for developing a disease or medical condition in an individual who does not currently have clinically apparent disease or the medical condition.

Note. The definitions are adapted from FDA-NIH Biomarker Working Group's BEST (Biomarkers, EndpointS, and other Tools) Resources [1].

Table S2. The list of research articles included in the literature survey (*N* = 57)

Reference	Measurement tool	Population	Clinical pain type	# of training models	# of independent tests
[19]	EEG	Clinical	Fibromyalgia(FM)	2	-
[36]	fMRI	Healthy	-	12	-
[40]	fMRI	Healthy	-	9	-
[6]	fMRI	Healthy	-	7	1
[4]	fMRI	Healthy	-	6	-
[45]	EEG	Healthy	-	5	-
[15]	EEG	Clinical	Chronic Pancreatitis	1	-
[55]	fMRI	Healthy	-	1	11
[2]	sMRI	Clinical	Chronic Pelvic Pain	2	-
[7]	fMRI	Clinical	Chronic Low Back Pain(cLBP)	1	-
[22]	sMRI	Clinical	Irritable Bowel Syndrome(IBS)	1	-
[14]	EEG	Healthy	-	2	-
[42]	sMRI	Clinical	Fibromyalgia(FM)	2	-
[48]	fMRI	Clinical	Osteoarthritis Pain(OA)	1	2
[50]	EEG+fMRI	Healthy	-	8	-
[17]	fMRI	Clinical	Fibromyalgia(FM)	2	1
[16]	fMRI	Clinical	Temporomandibular Disorders(TMD)	4	-
[32]	fMRI	Clinical	Fibromyalgia(FM)	2	5
[9]	fMRI	Clinical	Migraine	1	-
[52]	EEG	Healthy	-	2	-
[31]	fMRI	Healthy	-	-	1

(Supplementary Table 2 continues on the next page)

Reference	Measurement tool	Population	Clinical pain type	# of training models	# of independent tests
[29]	fMRI	Healthy	-	4	-
[57]	fMRI	Healthy	-	1	2
[37]	EEG	Healthy	-	2	-
[13]	EEG	Clinical	-	1	-
[53]	EEG	Clinical	Spinal cord injured	6	-
[28]	fMRI	Healthy	-	1	-
[59]	sMRI	Clinical	Trigeminal Neuralgia	1	-
[34]	fMRI	Clinical	Chronic Low Back Pain(cLBP)	4	2
[38]	EEG	Healthy	-	3	-
[11]	EEG	Healthy	-	1	-
[25]	EEG	Healthy	-	2	-
[46]	fMRI	Clinical	Chronic Low Back Pain(cLBP)	1	1
[23]	fMRI	Clinical	Chronic Low Back Pain(cLBP)	1	-
[44]	fMRI	Clinical	Fibromyalgia(FM), Back Pain	4	-
[43]	fMRI	Clinical	Neuropathic Pain	1	-
[39]	EEG	Clinical	Fibromyalgia(FM)	2	-
[49]	fMRI	Clinical	Chronic Low Back Pain(cLBP)	2	-
[20]	fMRI	Healthy	-	6	-
[30]	fMRI	Clinical	Knee osteoarthritis(KOA)	1	-
[8]	sMRI	Clinical	Primary Dysmenorrhea(PDM)	2	-
[58]	sMRI	Clinical	Herpes Zoster(HZ)	1	-

(Supplementary Table 2 continues on the next page)

Reference	Measurement tool	Population	Clinical pain type	# of training models	# of independent tests
[5]	EEG	Healthy	-	2	-
[47]	fMRI	Healthy	-	1	2
[10]	EEG	Clinical	Migraine	1	-
[35]	fMRI	Clinical	Irritable Bowel Syndrome(IBS)	4	4
[41]	fMRI	Clinical	Primary Dysmenorrhea(PDM)	1	-
[33]	fMRI	Clinical	Chronic Low Back Pain(cLBP)	1	2
[56]	EEG	Clinical	Herpes Zoster(HZ)	4	-
[12]	fMRI	Healthy	-	-	3
[18]	EEG	Healthy	-	4	-
[54]	fMRI	Healthy	-	5	-
[26]	fMRI	Healthy	-	9	-
[51]	sMRI	Clinical	Chronic Low Back Pain(cLBP)	1	-
[3]	fMRI	Clinical	Subacute Back Pain	1	1
[27]	fMRI	Healthy	-	4	2
[24]	fMRI	Healthy	-	1	8

Note. EEG, Electroencephalography; fMRI, functional Magnetic Resonance Imaging; sMRI, structural Magnetic Resonance Imaging

Table S3. Categories for the literature survey

Aspect	Categories
Measurement tool	EEG / sMRI / fMRI
Population	Clinical / Healthy
Prediction task	Binary classification / Multiclass classification / Regression
Target	Pain vs. no pain / Pain intensity / Pain sensitivity / Pain patients vs. controls / Pain persistence / Pain severity / Pain patient type / Treatment responder / Treatment effect / Pain site / Non-pain conditions
Model level	Idiographic model / Population-level model / Combination
Data level	TR level / TR-bin level / Trial level / Run level / Condition level / Individual level
Spatial scale	Single voxel / Single region / Combination of regions / Brain wide
Experimental task	Resting state / Phasic pain / Tonic pain / Structure
Feature type	Activation pattern / Activation mean / Connectivity pattern / Event Related Potentials / Time Frequency / Structural information
Algorithm	ANN / CNN / CVAE / DQDA / GPC / GPR / Decision tree / K-NN / LASSO-PCR / LDA / Linear Regression / Linear SVM / Linear SVR / Logistic regression / PLSR / Random Forest / RVM / RVR / SMO-SVM / the v-method / TPOT
Validation method	Holdout validation / K-fold CV / Leave-one-trial-out CV / Leave-one-run-out CV / Leave-one-participant-out CV / Leave-two-participant-out CV / Leave-three-participant-out CV
Sample size	Number of participants

Note. In the literature survey, we categorized models based on the listed categories. All models correspond to one category for each aspect. EEG, Electroencephalography; fMRI, functional Magnetic Resonance Imaging; sMRI, structural Magnetic Resonance Imaging; ANN, Artificial Neural Networks; CNN, Convolutional Neural Networks; CVAE, Conditional Variational Autoencoder; DQDA, Diagonal Quadratic Discriminate Analysis; GPC, Gaussian process classifier; GPR, Gaussian Process Regression; KNN, K-Nearest Neighbor; LASSO-PCR, the Least Absolute Shrinkage and Selection Operator Principal Component Regression; LDA, Linear Discriminant Analysis; SVM, Support vector machine; SVR, Support vector regression; PLSR, Partial Least Squares Regression; RVM, Relevance Vector Machine; RVR, Relevance Vector Regression; SMO-SVM, Sequential Minimum Optimization Support Vector Machine; CV, Cross-Validation

Table S4. Model performance for data levels

Benchmark	Train data level	Test data level	Binary Classification						Regression			
			Accuracy	Accuracy multi-level GLM	Sensitivity	Specificity	AUC	PPV	*r*	*r* multi-level GLM	RMSE	R^2
Train data level	no avg	no avg	85.05 ±1.31	beta = -1.09 *z* = -3.53 *p* = 0.00042 two-tailed, bootstrap test	87.53 ±2.52	82.56 ±2.44	95.44 ±0.84	85.72 ±1.61	0.6898 ±0.0117	beta = -0.03 *z* = -3.75 *p* = 0.00018 two-tailed, bootstrap test	0.1711 ±0.0070	-0.2985 ±0.1565
	2		84.53 ±1.32		86.58 ±2.60	82.47 ±2.37	95.45 ±0.75	85.16 ±1.48	0.6782 ±0.0178		0.1768 ±0.0073	-0.3907 ±0.1616
	4		83.17 ±1.43		85.82 ±2.86	80.50 ±2.62	95.04 ±0.86	83.88 ±1.58	0.6618 ±0.0180		0.1868 ±0.0077	-0.5845 ±0.1900
	8		81.70 ±1.44		85.73 ±2.79	77.64 ±3.06	94.23 ±0.88	82.45 ±1.74	0.6232 ±0.0197		0.2071 ±0.0094	-1.0013 ±0.2646
	16		80.31 ±1.45		84.58 ±2.94	76.03 ±2.93	92.91 ±0.85	80.44 ±1.61	0.5784 ±0.0231		0.2014 ±0.0080	-0.8452 ±0.2270
	no avg	16	93.75 ±2.17		95.45 ±3.18	92.05 ±3.23	100.00 ±0.00	94.84 ±2.01	0.9737 ±0.0036		0.1233 ±0.0087	-0.3647 ±0.2499
	2		93.75 ±2.17		94.32 ±3.34	93.18 ±3.08	100.00 ±0.00	95.63 ±1.89	0.9746 ±0.0031		0.1243 ±0.0091	-0.4015 ±0.2460
	4		93.18 ±2.35		92.05 ±3.96	94.32 ±2.92	100.00 ±0.00	96.34 ±1.80	0.9747 ±0.0033		0.1317 ±0.0096	-0.6263 ±0.2892
	8		90.34 ±2.72		92.05 ±3.96	88.64 ±4.26	100.00 ±0.00	93.09 ±2.47	0.9698 ±0.0043		0.1420 ±0.0119	-1.0094 ±0.3770
	16		89.77 ±2.73		89.77 ±4.17	89.77 ±4.17	100.00 ±0.00	93.90 ±2.38	0.9509 ±0.0092		0.1337 ±0.0102	-0.6608 ±0.2980

(Supplementary Table 4 continues on the next page)

Benchmark	Train data level	Test data level	Binary Classification						Regression			
			Accuracy	Accuracy multi-level GLM	Sensitivity	Specificity	AUC	PPV	*r*	*r* multi-level GLM	RMSE	R^2
Test data level	no avg	no avg	85.05 ±1.31		87.53 ±2.52	82.56 ±2.44	95.44 ±0.84	85.72 ±1.61	0.6898 ±0.0117		0.1711 ±0.0070	-0.2985 ±0.1565
		2	88.36 ±1.52	beta = 2.35 *z* = 3.43 *p* = 0.00061 two-tailed, bootstrap test	90.38 ±2.35	86.33 ±2.75	97.78 ±0.64	89.41 ±1.82	0.7542 ±0.0175	beta = 0.07 *z* = 4.43 *p* = 0.00001 two-tailed, bootstrap test	0.1571 ±0.0073	-0.3256 ±0.1866
		4	91.57 ±1.62		92.33 ±2.70	90.81 ±2.49	99.27 ±0.51	93.00 ±1.71	0.7903 ±0.0184		0.1473 ±0.0077	-0.4267 ±0.2173
		8	92.90 ±2.05		94.89 ±2.88	90.91 ±3.26	100.00 ±0.00	93.96 ±1.97	0.9235 ±0.0093		0.1291 ±0.0082	-0.3600 ±0.2354
		16	93.75 ±2.17		95.45 ±3.18	92.05 ±3.23	100.00 ±0.00	94.84 ±2.01	0.9737 ±0.0036		0.1233 ±0.0087	-0.3647 ±0.2499
	16	no avg	80.31 ±1.45		84.58 ±2.94	76.03 ±2.93	92.91 ±0.85	80.43 ±1.60	0.5784 ±0.0231		0.2013 ±0.0079	-0.8452 ±0.2269
		2	84.29 ±1.65	beta = 2.28 *z* = 3.40 *p* = 0.00068 two-tailed, bootstrap test	87.66 ±2.83	80.92 ±3.23	96.06 ±0.75	85.43 ±1.86	0.6633 ±0.0240	beta = 0.09 *z* = 3.93 *p* = 0.00009 two-tailed, bootstrap test	0.1802 ±0.0084	-0.7834 ±0.2498
		4	86.74 ±2.13		89.20 ±3.46	84.28 ±3.66	98.88 ±0.52	89.16 ±2.15	0.7334 ±0.0239		0.1629 ±0.0090	-0.8009 ±0.2823
		8	88.64 ±2.63		90.91 ±3.82	86.36 ±4.34	99.93 ±0.07	91.44 ±2.46	0.8720 ±0.0202		0.1416 ±0.0097	-0.6915 ±0.2901
		16	89.77 ±2.73		89.77 ±4.17	89.77 ±4.17	100 ±0.00	93.90 ±2.38	0.9509 ±0.0092		0.1336 ±0.010	-0.6608 ±0.2979

(Supplementary Table 4 continues on the next page)

Benchmark	Train data level	Test data level	Binary Classification						Regression			
			Accuracy	Accuracy multi-level GLM	Sensitivity	Specificity	AUC	PPV	*r*	*r* multi-level GLM	RMSE	R^2
Test data level (with matched # data across test data levels)	no avg	no avg	87.50 ±2.37	beta = 4.56 $z = 3.79$ $p = 0.00015$ two-tailed, bootstrap test	92.04 ±3.22	82.95 ±4.28	98.86 ±0.54	89.14 ±2.59	0.7806 ±0.0276	beta = 0.04 $z = 4.65$ $p = 0.000003$ two-tailed, bootstrap test	0.1589 ±0.0081	-1.0787 ±0.4316
		2	88.64 ±2.50		95.45 ±3.17	81.81 ±4.32	100.00 ±0.00	88.09 ±2.68	0.8522 ±0.0204		0.1553 ±0.0090	-0.9456 ±0.4052
		4	92.61 ±2.08		92.04 ±3.61	93.18 ±2.61	100.00 ±0.00	95.23 ±1.82	0.8871 ±0.0181		0.1479 ±0.0110	-0.7232 ±0.4057
		8	93.18 ±2.05		94.31 ±2.91	92.04 ±3.22	100.00 ±0.00	94.96 ±1.96	0.9556 ±0.0061		0.1261 ±0.0081	-0.4056 ±0.3440
		16	93.75 ±2.17		95.45 ±3.17	92.04 ±3.22	100.00 ±0.00	94.84 ±2.00	0.9737 ±0.0036		0.1233 ±0.0087	-0.3647 ±0.2499
	16	no avg	81.25 ±2.94	beta = 3.49 $z = 3.18$ $p = 0.00147$ two-tailed, bootstrap test	85.23 ±4.48	77.27 ±5.00	96.59 ±1.31	84.55 ±3.16	0.6498 ±0.0528	beta = 0.06 $z = 3.82$ $p = 0.00013$ two-tailed, bootstrap test	0.1887 ±0.0102	-1.9572 ±0.5072
		2	84.09 ±3.05		87.50 ±4.63	80.68 ±5.20	99.15 ±0.48	87.92 ±3.04	0.7995 ±0.0266		0.1823 ±0.0116	-1.6389 ±0.4568
		4	85.80 ±2.86		87.50 ±4.63	84.09 ±4.53	100.00 ±0.00	89.58 ±2.78	0.8650 ±0.0173		0.1595 ±0.0125	-0.9096 ±0.3439
		8	86.93 ±2.99		89.77 ±4.17	84.09 ±5.08	100.00 ±0.00	90.65 ±2.85	0.9240 ±0.0100		0.1410 ±0.0102	-0.7950 ±0.4213
		16	89.77 ±2.73		89.77 ±4.17	89.77 ±4.17	100.00 ±0.00	93.90 ±2.38	0.9509 ±0.0092		0.1337 ±0.0102	-0.6608 ±0.2980

Note. This table, related to Figure 7, displays performance metrics for different data levels, including the mean and standard error of the mean (s.e.m.). AUC, Area under the ROC curve; PPV, Positive Predictive Value; *r*, Pearson correlation between the actual and predicted values; RMSE, Root Mean Square Error; R^2, r-squared (or explained variance)

Table S5. Model performance for spatial scales

Spatial Scale		Binary Classification						Regression			
		Accuracy	Accuracy multi-level GLM Paired *t*-test	Sensitivity	Specificity	AUC	PPV	*r*	*r* multi-level GLM Paired *t*-test	RMSE	R^2
Number of Regions	1	68.79 ±4.92	beta = 4.25 *z* = 3.66 *p* = 0.00025 two-tailed, bootstrap test	67.44 ±13.42	70.13 ±10.90	80.58 ±5.53	71.54 ±5.37	0.4583 ±0.1048	beta = 0.06 *z* = 3.58 *p* = 0.00034 two-tailed, bootstrap test	0.177 ±0.0468	-0.5132 ±1.0586
	3	73.01 ±5.15		73.33 ±14.74	72.69 ±12.69	86.22 ±5.12	75.44 ±6.71	0.5658 ±0.1057		0.1737 ±0.0460	-0.5239 ±1.2164
	6	78.67 ±6.46		80.73 ±15.70	76.61 ±14.44	92.17 ±4.54	80.46 ±8.30	0.6242 ±0.1063		0.1717 ±0.0480	-0.5354 ±1.3468
	10	82.56 ±7.51		85.57 ±15.09	79.54 ±15.63	95.36 ±3.84	83.61 ±9.48	0.6663 ±0.1084		0.1707 ±0.0504	-0.5403 ±1.3986
	15	85.27 ±8.14		89.03 ±14.35	81.52 ±16.35	96.93 ±3.10	85.58 ±10.28	0.6973 ±0.1103		0.1694 ±0.0514	-0.5251 ±1.3922
Brain-wide masks	21	87.31 ±9.32	**21 vs. NP:** *t*(43) = 0.2882, *p* = 0.7746	91.59 ±13.76	83.03 ±18.21	97.6 ±2.66	86.84 ±11.89	0.7105 ±0.1231	**21 vs. NP:** *t*(43) = -0.7642, *p* = 0.4489	0.1685 ±0.0534	-0.5081 ±1.4036
	NP	86.96 ±8.92	**GM vs. NP:** *t*(43) = 0.9677, *p* = 0.3386	89.36 ±13.68	84.57 ±16.74	97.38 ±2.59	87.15 ±10.46	0.7227 ±0.0971	**GM vs. NP:** *t*(43) = -1.9625, *p* = 0.0562	0.1633 ±0.0553	-0.4317 ±1.3331
	GM	88.27 ±10.46	**GM vs. 21:** *t*(43) = 0.9808, *p* = 0.3322	89.51 ±17.79	87.03 ±18.06	97.96 ±3.27	89.98 ±11.68	0.7455 ±0.1196	**GM vs. 21:** *t*(43) = -2.6264, *p* = 0.0119	0.1613 ±0.0503	-0.4008 ±1.2535

Note. This table, related to Figure 8, displays performance metrics for different spatial scales, including the mean and standard deviation. AUC, Area under the ROC curve; PPV, Positive Predictive Value; *r*, Pearson correlation between the actual and predicted values; RMSE, Root Mean Square Error; R^2, r-squared (or explained variance)

Table S6. Model performance for model levels

Train	Test	Binary Classification							Regression		
		Accuracy	Accuracy Paired *t*-test	Sensitivity	Specificity	AUC	PPV	*r*	*r* Paired *t*-test	RMSE	R^2
Idiographic model	Within-individual run-level test	84.43 ±11.27	**Id vs. Po**: $t(120) = 0.2710$, $p = 0.7868$	82.99 ±14.80	85.86 ±16.84	94.56 ±7.00	87.21 ±13.96	0.6448 ±0.1844	**Id vs. Po**: $t(120) = -1.2872$, $p = 0.2005$	0.1241 ±0.0403	0.3592 ±0.2615
Population-level model		83.81 ±13.66		79.71 ±25.02	87.91 ±18.54	94.43 ±10.86	88.24 ±17.63	0.6875 ±0.1819		0.1569 ±0.0577	-0.2891 ±1.5668
Average of idiographic models	Independent test	86.76 ±6.30	**Avg Id vs. Po**: $t(86) = 1.1938$, $p = 0.2358$	85.79 ±10.08	87.74 ±8.07	92.08 ±5.47	87.96 ±7.01	0.6051 ±0.1252	**Avg Id vs. Po**: $t(86) = -2.8129$, $p = 0.0061$	0.1832 ±0.0661	-0.3567 ±1.0632
Population-level model		84.79 ±8.98		86.41 ±17.64	83.16 ±16.49	95.67 ±4.89	86.02 ±10.39	0.6807 ±0.1271		0.1732 ±0.0514	-0.3334 ±1.1137

Note. This table, related to Figure 9, displays performance metrics for different model levels, including the mean and standard deviation. AUC, Area under the ROC curve; PPV, Positive Predictive Value; *r*, Pearson correlation between the actual and predicted values; RMSE, Root Mean Square Error; R^2, r-squared (or explained variance)

Table S7. Model performance for sample sizes

Sample Size	Binary Classification						Regression			
	Accuracy	Accuracy multi-level GLM	Sensitivity	Specificity	AUC	PPV	*r*	*r* multi-level GLM	RMSE	R^2
10	83.50 ±0.58		81.12 ±3.44	85.88 ±2.67	96.18 ±0.70	87.88 ±1.59	0.6981 ±0.0164		0.1664 ±0.0051	-0.5135 ±0.1346
20	85.39 ±1.09		84.48 ±2.40	86.31 ±2.61	97.24 ±0.28	89.09 ±1.86	0.7266 ±0.0127		0.1638 ±0.0052	-0.4898 ±0.1333
30	85.94 ±0.83	beta = 0.68	85.84 ±1.95	86.04 ±2.79	97.49 ±0.28	88.54 ±2.21	0.7376 ±0.0099	beta = 0.01	0.1626 ±0.0046	-0.4640 ±0.1114
40	86.86 ±0.70	z = 3.96 p = 0.00008 two-tailed, bootstrap test	88.27 ±1.42	85.46 ±2.01	97.8 ±0.25	88.83 ±1.49	0.7412 ±0.0089	z = 4.02 p = 0.00006 two-tailed, bootstrap test	0.1621 ±0.0038	-0.4476 ±0.0887
50	87.15 ±0.40		88.39 ±1.43	85.91 ±2.03	97.88 ±0.22	89.09 ±1.61	0.7435 ±0.0073		0.1624 ±0.0039	-0.4452 ±0.0832
60	87.59 ±0.34		88.66 ±1.01	86.52 ±1.23	97.94 ±0.14	89.56 ±0.98	0.7449 ±0.0056		0.162 ±0.0028	-0.4306 ±0.0604
70	87.99 ±0.40		88.97 ±0.54	87.01 ±0.85	98.01 ±0.12	89.87 ±0.57	0.7455 ±0.0041		0.1615 ±0.0021	-0.4129 ±0.0444
80	88.27	-	89.51	87.03	97.96	89.98	0.7455	-	0.1613	-0.4008

Note. This table, related to Figure 10, displays performance metrics for different sample sizes, including the mean and standard deviation. AUC, Area under the ROC curve; PPV, Positive Predictive Value; *r*, Pearson correlation between the actual and predicted values; RMSE, Root Mean Square Error; R^2, r-squared (or explained variance

Supplemental References

[1] FDA-NIH Biomarker Working Group. BEST (Biomarkers, EndpointS, and other Tools) Resource. Silver Spring (MD), Bethesda (MD), 2016.

[2] Bagarinao E, Johnson KA, Martucci KT, Ichesco E, Farmer MA, Labus J, Ness TJ, Harris R, Deutsch G, Apkarian VA, Mayer EA, Clauw DJ, Mackey S. Preliminary structural MRI based brain classification of chronic pelvic pain: A MAPP network study. Pain 2014;155(12):2502-2509.

[3] Baliki MN, Petre B, Torbey S, Herrmann KM, Huang L, Schnitzer TJ, Fields HL, Apkarian AV. Corticostriatal functional connectivity predicts transition to chronic back pain. Nat Neurosci 2012;15(8):1117-1119.

[4] Brodersen KH, Wiech K, Lomakina EI, Lin CS, Buhmann JM, Bingel U, Ploner M, Stephan KE, Tracey I. Decoding the perception of pain from fMRI using multivariate pattern analysis. Neuroimage 2012;63(3):1162-1170.

[5] Brown CA, Almarzouki AF, Brown RJ, Jones AKP. Neural representations of aversive value encoding in pain catastrophizers. Neuroimage 2019;184:508-519.

[6] Brown JE, Chatterjee N, Younger J, Mackey S. Towards a physiology-based measure of pain: patterns of human brain activity distinguish painful from non-painful thermal stimulation. PLoS One 2011;6(9):e24124.

[7] Callan D, Mills L, Nott C, England R, England S. A tool for classifying individuals with chronic back pain: using multivariate pattern analysis with functional magnetic resonance imaging data. PLoS One 2014;9(6):e98007.

[8] Chen T, Mu J, Xue Q, Yang L, Dun W, Zhang M, Liu J. Whole-brain structural magnetic resonance imaging-based classification of primary dysmenorrhea in pain-free phase: a machine learning study. Pain 2019;160(3):734-741.

[9] Chong CD, Gaw N, Fu Y, Li J, Wu T, Schwedt TJ. Migraine classification using magnetic resonance imaging resting-state functional connectivity data. Cephalalgia 2017;37(9):828-844.

[10] Frid A, Shor M, Shifrin A, Yarnitsky D, Granovsky Y. A Biomarker for Discriminating Between Migraine With and Without Aura: Machine Learning on Functional Connectivity on Resting-State EEGs. Ann Biomed Eng 2020;48(1):403-412.

[11] Furman AJ, Meeker TJ, Rietschel JC, Yoo S, Muthulingam J, Prokhorenko M, Keaser ML, Goodman RN, Mazaheri A, Seminowicz DA. Cerebral peak alpha frequency predicts individual differences in pain sensitivity. Neuroimage 2018;167:203-210.

[12] Geuter S, Reynolds Losin EA, Roy M, Atlas LY, Schmidt L, Krishnan A, Koban L, Wager TD, Lindquist MA. Multiple Brain Networks Mediating Stimulus-Pain Relationships in Humans. Cereb Cortex 2020;30(7):4204-4219.

[13] Gram M, Erlenwein J, Petzke F, Falla D, Przemeck M, Emons MI, Reuster M, Olesen SS, Drewes AM. Prediction of postoperative opioid analgesia using clinical-experimental parameters and electroencephalography. Eur J Pain 2017;21(2):264-277.

[14] Gram M, Graversen C, Olesen AE, Drewes AM. Machine learning on encephalographic activity may predict opioid analgesia. Eur J Pain 2015;19(10):1552-1561.

[15] Graversen C, Olesen SS, Olesen AE, Steimle K, Farina D, Wilder-Smith OH, Bouwense SA, van Goor H, Drewes AM. The analgesic effect of pregabalin in patients with chronic pain is reflected by changes in pharmaco-EEG spectral indices. Br J Clin Pharmacol 2012;73(3):363-372.

[16] Harper DE, Shah Y, Ichesco E, Gerstner GE, Peltier SJ. Multivariate classification of pain-

evoked brain activity in temporomandibular disorder. Pain Rep 2016;1(3).
[17] Harte SE, Ichesco E, Hampson JP, Peltier SJ, Schmidt-Wilcke T, Clauw DJ, Harris RE. Pharmacologic attenuation of cross-modal sensory augmentation within the chronic pain insula. Pain 2016;157(9):1933-1945.
[18] Huang G, Xiao P, Hung YS, Iannetti GD, Zhang ZG, Hu L. A novel approach to predict subjective pain perception from single-trial laser-evoked potentials. Neuroimage 2013;81:283-293.
[19] Hunter AM, Leuchter AF, Cook IA, Abrams M, Siegman BE, Furst DE, Chappell AS. Brain functional changes and duloxetine treatment response in fibromyalgia: a pilot study. Pain Med 2009;10(4):730-738.
[20] Jung WM, Lee IS, Lee YS, Kim J, Park HJ, Wallraven C, Chae Y. Decoding spatial location of perceived pain to acupuncture needle using multivoxel pattern analysis. Mol Pain 2019;15:1744806919877060.
[21] Kohoutova L, Atlas LY, Buchel C, Buhle JT, Geuter S, Jepma M, Koban L, Krishnan A, Lee DH, Lee S, Roy M, Schafer SM, Schmidt L, Wager TD, Woo CW. Individual variability in brain representations of pain. Nat Neurosci 2022;25(6):749-759.
[22] Labus JS, Van Horn JD, Gupta A, Alaverdyan M, Torgerson C, Ashe-McNalley C, Irimia A, Hong JY, Naliboff B, Tillisch K, Mayer EA. Multivariate morphological brain signatures predict patients with chronic abdominal pain from healthy control subjects. Pain 2015;156(8):1545-1554.
[23] Lee J, Mawla I, Kim J, Loggia ML, Ortiz A, Jung C, Chan ST, Gerber J, Schmithorst VJ, Edwards RR, Wasan AD, Berna C, Kong J, Kaptchuk TJ, Gollub RL, Rosen BR, Napadow V. Machine learning-based prediction of clinical pain using multimodal neuroimaging and autonomic metrics. Pain 2019;160(3):550-560.
[24] Lee JJ, Kim HJ, Ceko M, Park BY, Lee SA, Park H, Roy M, Kim SG, Wager TD, Woo CW. A neuroimaging biomarker for sustained experimental and clinical pain. Nat Med 2021;27(1):174-182.
[25] Li L, Huang G, Lin Q, Liu J, Zhang S, Zhang Z. Magnitude and Temporal Variability of Inter-stimulus EEG Modulate the Linear Relationship Between Laser-Evoked Potentials and Fast-Pain Perception. Front Neurosci 2018;12:340.
[26] Liang M, Mouraux A, Hu L, Iannetti GD. Primary sensory cortices contain distinguishable spatial patterns of activity for each sense. Nat Commun 2013;4:1979.
[27] Liang M, Su Q, Mouraux A, Iannetti GD. Spatial Patterns of Brain Activity Preferentially Reflecting Transient Pain and Stimulus Intensity. Cereb Cortex 2019;29(5):2211-2227.
[28] Lin Q, Li L, Liu J, Liu W, Huang G, Zhang Z. Influence of Individual Differences in fMRI-Based Pain Prediction Models on Between-Individual Prediction Performance. Front Neurosci 2018;12:569.
[29] Lindquist MA, Krishnan A, Lopez-Sola M, Jepma M, Woo CW, Koban L, Roy M, Atlas LY, Schmidt L, Chang LJ, Reynolds Losin EA, Eisenbarth H, Ashar YK, Delk E, Wager TD. Group-regularized individual prediction: theory and application to pain. Neuroimage 2017;145(Pt B):274-287.
[30] Liu J, Chen L, Tu Y, Chen X, Hu K, Tu Y, Lin M, Xie G, Chen S, Huang J, Liu W, Wu J, Xiao T, Wilson G, Lang C, Park J, Tao J, Kong J. Different exercise modalities relieve pain syndrome in patients with knee osteoarthritis and modulate the dorsolateral prefrontal cortex: A multiple mode MRI study. Brain Behav Immun 2019;82:253-263.
[31] Lopez-Sola M, Koban L, Krishnan A, Wager TD. When pain really matters: A vicarious-pain

brain marker tracks empathy for pain in the romantic partner. Neuropsychologia 2020;145:106427.
[32] Lopez-Sola M, Woo CW, Pujol J, Deus J, Harrison BJ, Monfort J, Wager TD. Towards a neurophysiological signature for fibromyalgia. Pain 2017;158(1):34-47.
[33] Makary MM, Polosecki P, Cecchi GA, DeAraujo IE, Barron DS, Constable TR, Whang PG, Thomas DA, Mowafi H, Small DM, Geha P. Loss of nucleus accumbens low-frequency fluctuations is a signature of chronic pain. Proc Natl Acad Sci U S A 2020;117(18):10015-10023.
[34] Mano H, Kotecha G, Leibnitz K, Matsubara T, Sprenger C, Nakae A, Shenker N, Shibata M, Voon V, Yoshida W, Lee M, Yanagida T, Kawato M, Rosa MJ, Seymour B. Classification and characterisation of brain network changes in chronic back pain: A multicenter study. Wellcome Open Res 2018;3:19.
[35] Mao CP, Chen FR, Huo JH, Zhang L, Zhang GR, Zhang B, Zhou XQ. Altered resting-state functional connectivity and effective connectivity of the habenula in irritable bowel syndrome: A cross-sectional and machine learning study. Hum Brain Mapp 2020;41(13):3655-3666.
[36] Marquand A, Howard M, Brammer M, Chu C, Coen S, Mourao-Miranda J. Quantitative prediction of subjective pain intensity from whole-brain fMRI data using Gaussian processes. Neuroimage 2010;49(3):2178-2189.
[37] Misra G, Wang WE, Archer DB, Roy A, Coombes SA. Automated classification of pain perception using high-density electroencephalography data. J Neurophysiol 2017;117(2):786-795.
[38] Okolo C, Omurtag A. Research: Use of Dry Electroencephalogram and Support Vector for Objective Pain Assessment. Biomed Instrum Technol 2018;52(5):372-378.
[39] Paul JK, Iype T, R D, Hagiwara Y, Koh JW, Acharya UR. Characterization of fibromyalgia using sleep EEG signals with nonlinear dynamical features. Comput Biol Med 2019;111:103331.
[40] Prato M, Favilla S, Zanni L, Porro CA, Baraldi P. A regularization algorithm for decoding perceptual temporal profiles from fMRI data. Neuroimage 2011;56(1):258-267.
[41] Quan S, Yang J, Dun W, Wang K, Liu H, Liu J. Prediction of pain intensity with uterine morphological features and brain microstructural and functional properties in women with primary dysmenorrhea. Brain Imaging Behav 2021;15(3):1580-1588.
[42] Robinson ME, O'Shea AM, Craggs JG, Price DD, Letzen JE, Staud R. Comparison of machine classification algorithms for fibromyalgia: neuroimages versus self-report. J Pain 2015;16(5):472-477.
[43] Rogachov A, Bhatia A, Cheng JC, Bosma RL, Kim JA, Osborne NR, Hemington KS, Venkatraghavan L, Davis KD. Plasticity in the dynamic pain connectome associated with ketamine-induced neuropathic pain relief. Pain 2019;160(7):1670-1679.
[44] Santana AN, Cifre I, de Santana CN, Montoya P. Using Deep Learning and Resting-State fMRI to Classify Chronic Pain Conditions. Front Neurosci 2019;13:1313.
[45] Schulz E, Zherdin A, Tiemann L, Plant C, Ploner M. Decoding an individual's sensitivity to pain from the multivariate analysis of EEG data. Cereb Cortex 2012;22(5):1118-1123.
[46] Shen W, Tu Y, Gollub RL, Ortiz A, Napadow V, Yu S, Wilson G, Park J, Lang C, Jung M, Gerber J, Mawla I, Chan ST, Wasan AD, Edwards RR, Kaptchuk T, Li S, Rosen B, Kong J. Visual network alterations in brain functional connectivity in chronic low back pain: A resting state functional connectivity and machine learning study. Neuroimage Clin

2019;22:101775.
[47] Spisak T, Kincses B, Schlitt F, Zunhammer M, Schmidt-Wilcke T, Kincses ZT, Bingel U. Pain-free resting-state functional brain connectivity predicts individual pain sensitivity. Nat Commun 2020;11(1):187.
[48] Tetreault P, Mansour A, Vachon-Presseau E, Schnitzer TJ, Apkarian AV, Baliki MN. Brain Connectivity Predicts Placebo Response across Chronic Pain Clinical Trials. PLoS Biol 2016;14(10):e1002570.
[49] Tu Y, Ortiz A, Gollub RL, Cao J, Gerber J, Lang C, Park J, Wilson G, Shen W, Chan ST, Wasan AD, Edwards RR, Napadow V, Kaptchuk TJ, Rosen B, Kong J. Multivariate resting-state functional connectivity predicts responses to real and sham acupuncture treatment in chronic low back pain. Neuroimage Clin 2019;23:101885.
[50] Tu Y, Tan A, Bai Y, Hung YS, Zhang Z. Decoding Subjective Intensity of Nociceptive Pain from Pre-stimulus and Post-stimulus Brain Activities. Front Comput Neurosci 2016;10:32.
[51] Ung H, Brown JE, Johnson KA, Younger J, Hush J, Mackey S. Multivariate classification of structural MRI data detects chronic low back pain. Cereb Cortex 2014;24(4):1037-1044.
[52] Vijayakumar V, Case M, Shirinpour S, He B. Quantifying and Characterizing Tonic Thermal Pain Across Subjects From EEG Data Using Random Forest Models. IEEE Trans Biomed Eng 2017;64(12):2988-2996.
[53] Vuckovic A, Gallardo VJF, Jarjees M, Fraser M, Purcell M. Prediction of central neuropathic pain in spinal cord injury based on EEG classifier. Clin Neurophysiol 2018;129(8):1605-1617.
[54] Wager TD, Atlas LY, Leotti LA, Rilling JK. Predicting individual differences in placebo analgesia: contributions of brain activity during anticipation and pain experience. J Neurosci 2011;31(2):439-452.
[55] Wager TD, Atlas LY, Lindquist MA, Roy M, Woo CW, Kross E. An fMRI-based neurologic signature of physical pain. N Engl J Med 2013;368(15):1388-1397.
[56] Wei M, Liao Y, Liu J, Li L, Huang G, Huang J, Li D, Xiao L, Zhang Z. EEG Beta-Band Spectral Entropy Can Predict the Effect of Drug Treatment on Pain in Patients With Herpes Zoster. J Clin Neurophysiol 2022;39(2):166-173.
[57] Woo CW, Schmidt L, Krishnan A, Jepma M, Roy M, Lindquist MA, Atlas LY, Wager TD. Quantifying cerebral contributions to pain beyond nociception. Nat Commun 2017;8:14211.
[58] Zeng P, Huang J, Wu S, Qian C, Chen F, Sun W, Tao W, Liao Y, Zhang J, Yang Z, Zhong S, Zhang Z, Xiao L, Huang B. Characterizing the Structural Pattern Predicting Medication Response in Herpes Zoster Patients Using Multivoxel Pattern Analysis. Front Neurosci 2019;13:534.
[59] Zhong J, Chen DQ, Hung PS, Hayes DJ, Liang KE, Davis KD, Hodaie M. Multivariate pattern classification of brain white matter connectivity predicts classic trigeminal neuralgia. Pain 2018;159(10):2076-2087.